第 48 卷 第 19 期/2021 年 10 月/中国激光 特邀论文

中国激光

基于 Lyot 滤波器的脉冲态可切换掺镱光纤激光器

林彦吕[1,2,3]，黄梓楠[1,2,3]，黄千千[1,2,3]，戴礼龙[1,2,3]，邢志坤[4]，闫志君[4]，牟成博[1,2,3*]

[1]上海大学通信与信息工程学院特种光纤与光接入网重点实验室，上海 200444；

[2]上海大学上海先进通信与数据科学研究院，上海 200444；

[3]上海大学特种光纤与先进通信国际合作联合实验室，上海 200444；

[4]华中科技大学光学与电子信息学院下一代互联网接入系统国家工程实验室，湖北 武汉 430074

摘要 采用由一对保偏 45°倾斜光纤光栅构成的 Lyot 滤波器，设计了一台脉冲态可切换的掺镱光纤激光器。该 Lyot 滤波器集成了起偏器和梳状滤波器的功能，为激光器实现耗散孤子锁模提供了光谱滤波效应，从而使激光器产生了中心波长为 1038.82 nm、脉冲宽度为 5.2 ps 的耗散孤子脉冲。随着泵浦功率的增加，非线性偏振旋转反馈机制的切换导致激光器的锁模脉冲态发生了耗散孤子脉冲与类噪声脉冲之间的多重切换。脉冲态切换过程中仅需调节泵浦功率，而不需要改变偏振控制器的状态。该脉冲态可切换激光器可以用于设计更精准可控的多功能光源。

关键词 光栅；光束传输；倾斜光纤光栅；掺镱光纤激光器；非线性偏振旋转；耗散孤子

中图分类号 TN284 **文献标志码** A **doi**：10.3788/CJL202148.1901004

1 引 言

由于可以产生超短脉冲，并且可以为研究孤子脉冲动力学过程提供绝佳的平台，近年来，被动锁模光纤激光器受到了越来越多研究学者的关注。目前的被动锁模光纤激光器，根据色散在谐振腔内分布位置的不同，形成了多种不同的脉冲整形机制，如经典孤子[1]、展宽脉冲[2]、自相似子[3]及耗散孤子[4]等。孤子脉冲的发展历程将单脉冲能量提升到了新的量级，使得光纤激光器迎合了更多领域的需求，如光学计量[5]、生物医学[6]和激光微加工[7]等。

耗散孤子通常产生于较大净正色散的激光器中，是色散、非线性、增益和损耗共同作用的结果[8]。研究表明，由光谱滤波效应引入的光谱幅度调制是形成耗散孤子的关键[9]。为了在激光器中引入光谱滤波效应，学者们在谐振腔中引入了多种类型的滤波器，如 Sagnac 干涉仪[10]、啁啾光纤光栅[11]、双折射滤波器[12]等。其中，双折射滤波器具有滤波带宽可调、结构简单、光纤兼容性好的优点，备受研究学者们的青睐。Lin 等[13]设计了一种基于光纤弱双折射的双折射滤波器，在全正色散掺镱光纤激光器中实现了稳定的耗散孤子锁模。Zhang 等[14]将保偏光纤作为强双折射介质，在全正色散的掺镱光纤激光器中形成了耗散孤子脉冲。虽然这些结构的双折射滤波器在激光器中得到了广泛的应用，但其梳状滤波的形成以及强弱都与偏振控制器的调节相关。毫无疑问，偏振控制器固有的偏振敏感性限制了激光器的发展，同时也影响了激光器锁模的稳定。因此，寻求一种具有强稳定滤波的双折射滤波器成为了目前的研究热点之一。

此外，在正色散区域的激光器中，除了耗散孤子，类噪声脉冲同样得到了广泛的研究。类噪声脉冲具有超宽的光谱，可以用于产生超连续谱、扫描光谱域光学相干断层[15]等。众多研究表明，类噪声脉冲更容易在高泵浦功率条件下产生。通过合理调节谐振腔内的参数，如泵浦功率，可以同时在全正色散

收稿日期：2021-06-18；**修回日期**：2021-07-09；**录用日期**：2021-08-16

基金项目：国家自然科学基金(61975107，62075071)、上海市自然科学基金(20ZR1471500)、中国科学院空间主动光电技术重点实验室开放课题(2021-ZDKF-1)

通信作者：*mouc1@shu.edu.cn

的掺镱光纤激光器中产生耗散孤子与类噪声脉冲[16-17]。Sobon 等[18]在掺铥光纤激光器实现耗散孤子锁模的同时，通过增加泵浦功率，锁模激光器实现了从耗散孤子到类噪声脉冲的脉冲态切换。Li 等[19]同样采用增加泵浦功率的方式，在掺镱光纤激光器中实现了耗散孤子与类噪声脉冲的切换运行。脉冲态切换虽然在众多实验中得到了验证，但在掺镱光纤激光器中，有关耗散孤子与类噪声脉冲的多重切换鲜有报道。

本文利用一对保偏 45°倾斜光纤光栅作为起偏器，一段保偏光纤作为双折射介质，设计出了一种具有稳定强滤波效应的 Lyot 滤波器。将该滤波器作为光谱滤波器应用于全正色散的掺镱光纤激光器中，激光器实现了稳定的耗散孤子锁模。并在耗散孤子锁模状态下，通过单向调节泵浦功率，激光器实现了耗散孤子脉冲—类噪声脉冲—耗散孤子脉冲的脉冲态切换，这种脉冲态的多重切换在掺镱光纤激光器中鲜有报道。值得一提的是，全部切换过程不需要调节偏振控制器，这种可以产生多种脉冲态的激光器具备成为精准可控的多功能光源的潜力。

2 实验装置

实验所用的 Lyot 滤波器由两个保偏 45°倾斜光纤光栅和一段保偏光纤组成。其中，倾斜光栅以特殊的拼接角分别熔接在保偏光纤的两端，这种特殊结构使其在激光器谐振腔中不仅可以作为梳状滤波器，还可以作为光纤型的起偏器。保偏 45°倾斜光纤光栅是采用紫外相位掩模版扫描技术，在保偏光纤的主轴（快轴或慢轴）上刻写制备的。更多有关这种 Lyot 滤波器和保偏 45°倾斜光纤光栅的制作细节已经报道在了文献[20-21]中。Lyot 滤波器的原理图如图 1(a)所示。第一个保偏 45°倾斜光纤光栅将 TE 偏振分量耦合出纤芯，并使 TM 偏振分量在光纤纤芯中传播以产生线偏振光[20]。由于保偏 45°倾斜光纤光栅与保偏光纤之间特殊的熔接角，线偏振光将在保偏光纤中积累一定的线性相移。偏振光所积累的线性相移将在第二个保偏 45°倾斜光纤光栅中转换为幅度调制，最终产生梳状滤波。为了使滤波器具有最大的滤波调制深度，保偏 45°倾斜光纤光栅与保偏光纤之间的拼接角设计为 45°。该滤波器传输谱如图 1(b)所示，长度约为 24 cm 的保偏光纤决定了滤波器的自由光谱范围约为 10.2 nm，相应的滤波带宽为 5.1 nm。

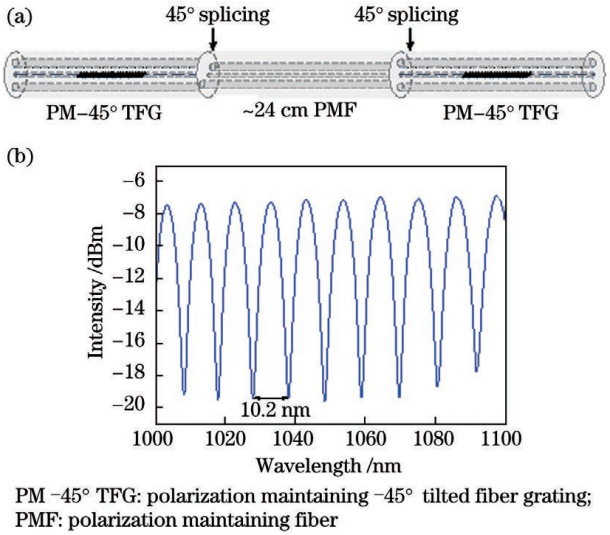

图 1 Lyot 滤波器。(a)原理图；(b)传输谱

Fig. 1 Lyot filter. (a) Schematic diagram; (b) transmission spectrum

锁模脉冲态可切换的掺镱光纤激光器原理图如图 2 所示。一段 96 cm 长的掺镱光纤（Yb1200-4/125，Liekki）作为增益介质，由一台 980 nm 的台式泵浦源（CLD1015，Thorlabs）通过波分复用器对其进行泵浦。一个 10∶90 的耦合器放置在了增益光纤之后，用以输出 10%的激光。Lyot 滤波器在实现梳状滤波功能的同时，还可以作为起偏器提供起偏的功能。将该滤波器放置在两个偏振控制器之间，可以与两个偏振控制器共同构成人造式可饱和吸收体，实现激光器的非线性偏振旋转锁模。同时，该滤波器提供了 10.2 nm 的自由光谱范围以及相应的 5.1 nm 的滤波带宽。隔离器保证了激光在谐振腔中的单向传输。谐振腔的总腔长约为 9 m，实验中所用的光纤和器件均为正常色散。10%的输出激光将用于检测激光器的光学特性。其中，激光光谱、时

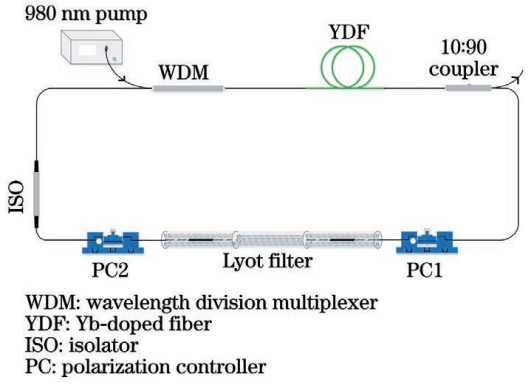

图 2 基于 Lyot 滤波器的掺镱光纤激光器原理图

Fig. 2 Schematic diagram of Yb-doped fiber laser based on Lyot filter

域脉冲序列、射频谱和自相关曲线将分别采用光谱仪(AQ6370B,Yokogawa)、采样率为 40 GSa/s 的示波器(DSO90804A,Keysight)、射频仪(SSA3032X,Siglent)和自相关仪(PulseCheck600,A. P. E)进行记录。同时,实验中还使用了光电探测器(818-BB-51F,Newport)进行光电转换。

3 分析与讨论

由于实验所用的 Lyot 滤波器可以产生强梳状滤波,提供了全正色散激光器实现耗散孤子锁模所需的光谱滤波效应,同时其稳定的滤波使激光器具有较低的锁模阈值功率。将泵浦功率缓慢增加至 177 mW,并仔细地调节偏振控制器,激光器即可实现稳定的耗散孤子锁模,脉冲特性如图 3 所示。图 3(a)为脉冲光谱,从图中可以看出,耗散孤子中心波长 λ_c 为 1038.82 nm,3 dB 带宽为 11.76 nm。光谱具有边沿陡峭、顶部平坦的类矩形状,是耗散孤子的典型特征。此外,光谱两侧具有明显的边带,是滤波器周期性滤波所引起的[22]。图 3(b)给出了重复周期为 35.16 ns 的时域脉冲序列,相应的脉冲重复频率为 28.44 MHz,与激光器的谐振腔腔长相吻合。图 3(c)为耗散孤子脉冲的自相关(AC)曲线,采用高斯函数对其进行拟合,测量所得的脉冲宽度约为 5.2 ps,时间带宽积为 17.00,表明脉冲具有较大的啁啾。图 3(d)给出了扫描带宽为 1 MHz、采样率为 1 kHz 的射频谱,可以得到脉冲的信噪比约为 53 dB,插图中 3.2 GHz 扫描带宽的射频谱没有明显频率调制,表明此时锁模所产生的耗散孤子脉冲具有较好的稳定性。在这一泵浦功率下,激光器的输出平均功率为 5.3 mW。

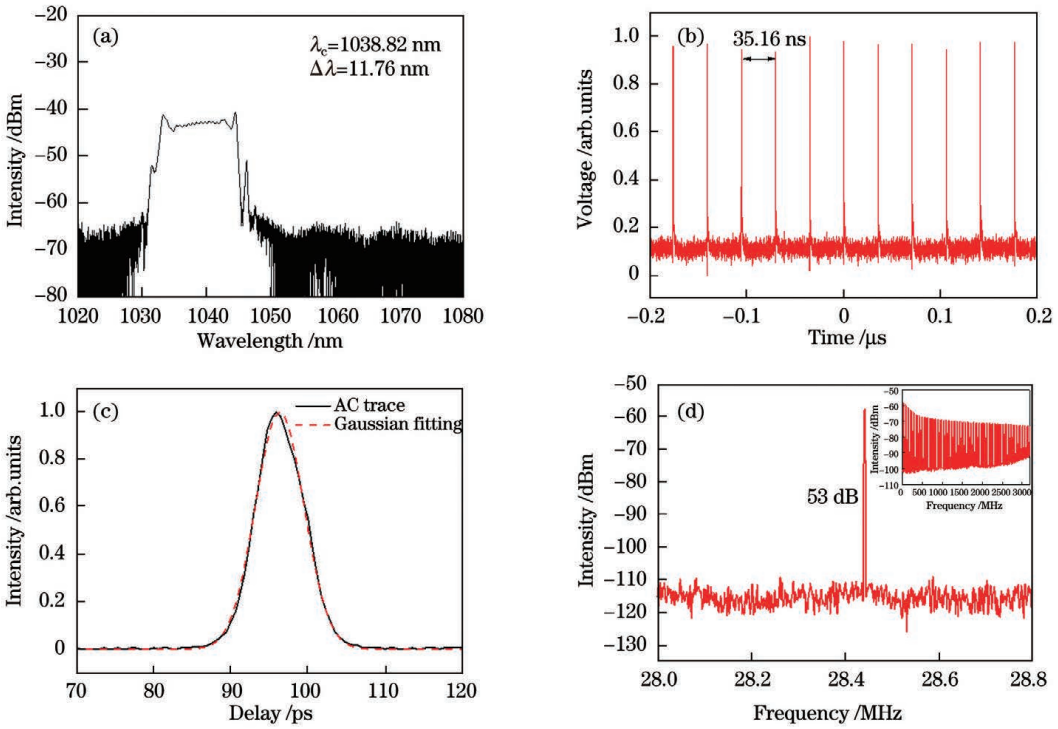

图 3 泵浦功率为 177 mW 时的耗散孤子脉冲特性。(a)光谱图;(b)时域脉冲序列;(c)自相关曲线;(d)射频谱,插图是扫描带宽为 3.2 GHz 的射频谱

Fig. 3 Characteristics of dissipative soliton pulse under pump power of 177 mW. (a) Spectrum; (b) time domain pulse sequence; (c) autocorrelation curve; (d) radio frequency spectrum, inset is radio frequency spectrum with scanning bandwidth of 3.2 GHz

实验中,通过改变激光器的泵浦功率,还可以观察到类噪声脉冲的产生。在 177 mW 的泵浦功率下,通过调节偏振控制器,激光器实现了稳定的耗散孤子锁模,光谱和自相关曲线如图 4(a)和图 4(b)所示。在这一锁模状态下,保持偏振控制器的状态不变,仅通过增加泵浦功率,即可观察到激光器锁模脉冲态的切换。当泵浦功率增加到 323 mW 时,受到增强的自相位调制效应的影响,光谱逐渐展宽,如图 4(c)所示,光谱 3 dB 带宽为 12.47 nm。此时激光器产生的脉冲仍为耗散孤子,但增强的非线性效应使得光谱两侧边带明显增加[23],同时光谱顶部出现了周期性振荡的条纹。从图4(d)中的自相关曲

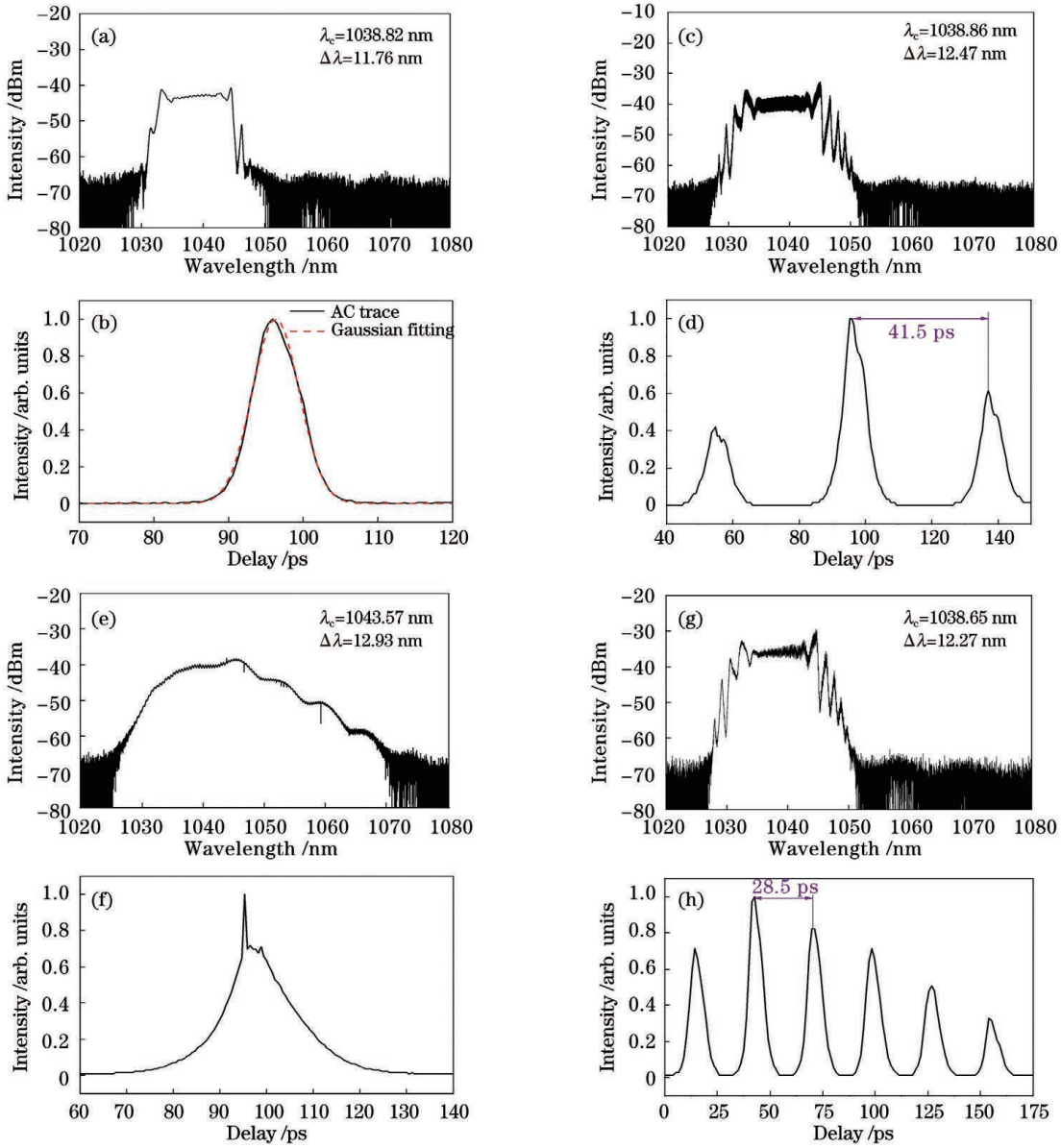

图 4 不同泵浦功率下的锁模脉冲特性。(a)(b)177 mW 时的光谱图和自相关曲线;(c)(d)323 mW 时的光谱图和自相关曲线;(e)(f)455 mW 时的光谱图和自相关曲线;(g)(h)691 mW 时的光谱图和自相关曲线

Fig. 4 Characteristics of mode-locked pulse under different pump power. (a)(b) Spectrum and autocorrelation trace at 177 mW; (c)(d) spectrum and autocorrelation trace at 323 mW; (e)(f) spectrum and autocorrelation trace at 455 mW; (g)(h) spectrum and autocorrelation trace at 691 mW

线可以看出,主脉冲的两侧对称分布着两个附属脉冲,主脉冲与附属脉冲之间的时间间隔约为 41.5 ps,因此可以得知,此时激光器产生了束缚态的耗散孤子脉冲。继续增加泵浦功率至 455 mW,从图 4(e)中可以看出,光谱陡峭的边沿消失,并且逐渐展宽变得平滑。图 4(f)中的自相关曲线显示了一个宽底座窄尖峰的结构,与类噪声脉冲的典型特征一致,说明此时激光器工作在了类噪声脉冲机制。当继续增加泵浦功率达到 691 mW 时,激光器又再次产生耗散孤子脉冲,此时的光谱如图 4(g)所示。在高非线性效应的影响下,此时锁模产生的耗散孤子脉冲依旧为束缚态,并且分裂出了更多的附属脉冲,如图 4(h)的自相关曲线所示,主脉冲与附属脉冲之间的时间间隔为 28.5 ps。一般来说,束缚态脉冲的自相关曲线通常具有对称性,但受到自相关仪扫描范围的限制,实验中无法记录完整的自相关曲线,图 4(h)仅显示了部分的自相关数据。由于实验中所用的泵浦源最多提供 691 mW 的泵浦功率,因此无法继续观测在更高的泵浦功率下激光器脉冲态的演化情

况。在 691 mW 的浦功率下，激光器的输出平均功率达到了 37.1 mW。受到耗散孤子迟滞效应的影响，在降低泵浦功率过程中，激光器一直处于耗散孤子状态，并未发生耗散孤子与类噪声脉冲之间的切换。但重新增加泵浦功率时，激光器又将产生耗散孤子—类噪声脉冲—耗散孤子的切换，这是一个可重复过程。

在实验中，保持偏振控制器状态不变，通过改变泵浦功率，激光器实现了耗散孤子与类噪声脉冲之间的脉冲态切换。这种脉冲态的切换与非线性偏振旋转的反馈机制相关。非线性偏振旋转的传输函数[24]可以表示为

$$|T_{\mathrm{NPR}}|^2=\sin^2\theta\sin^2\Psi+\cos^2\theta\cos^2\Psi+\frac{1}{2}\sin(2\theta)\sin(2\Psi)\cos(\Delta\varphi_{\mathrm{L}}+\Delta\varphi_{\mathrm{NL}}),\tag{1}$$

式中：θ 表示光纤 x 轴和起偏器之间的夹角；Ψ 表示光纤 y 轴和起偏器之间的夹角；线性相移 $\Delta\varphi_{\mathrm{L}}=\Delta\varphi_0+2\pi(1-\Delta\lambda/\lambda)L/L_{\mathrm{b}}$，其中 $\Delta\varphi_0$ 为光纤中两个正交模式的初始相位差，λ 为脉冲中心波长，$\Delta\lambda$ 是相对于中心波长 λ 的偏移量，L 是双折射光纤长度，L_{b} 是双折射光纤拍长；非线性相移 $\Delta\varphi_{\mathrm{NL}}=2\gamma LP\cos(2\theta)/3$，其中 γ 为光纤的非线性系数，P 为脉冲的瞬时功率。

在获得稳定的耗散孤子锁模后，保持偏振控制器的状态不变，当泵浦功率逐渐增加时，脉冲峰值功率也随之增加，就使得谐振腔内的瞬时功率 P 逐渐增大。瞬时功率的增大改变了腔内的非线性相移，进而影响了非线性偏振旋转的传输谱。图 5 显示了瞬时功率与非线性偏振旋转透过率的关系曲线，正弦状的传输谱意味着非线性偏振旋转存在正反馈和负反馈两种不同的状态。在正反馈机制中，非线性偏振旋转的透过率随着瞬时功率 P 的增加而增加；而在负反馈机制中，非线性偏振旋转的透过率随着瞬时功率 P 的增加而减小。正负反馈之间的临界瞬时功率称为临界饱和功率(CSP)，即图 5 中透过率的最大值与最小值。当腔内瞬时功率超过临界饱和功率时，非线性偏振旋转的反馈机制将从一种状态切换为另一种状态。这就使得实验中激光器在处于较低的泵浦功率时，非线性偏振旋转处于正反馈状态，此时激光器通过锁模产生了耗散孤子脉冲。在实现稳定锁模后，随着泵浦功率的不断提升，锁模脉冲的峰值功率也不断增加，使得腔内的瞬时功率也逐渐增强。当腔内的瞬时功率超过临界饱和功率时，非线性偏振旋转的反馈机制从正反馈状态切换到了负反馈状态。反馈机制的切换使得激光器的锁模脉冲态从耗散孤子脉冲切换到了类噪声脉冲。继续增加泵浦功率，由于腔内瞬时功率使非线性偏振旋转一直处于负反馈状态，激光器在这一泵浦功率范围内产生的脉冲均为类噪声脉冲。当瞬时功率再次达到临界饱和功率时，反馈机制从负反馈状态切换回了正反馈状态，使得激光器的锁模脉冲态也再次切换回了耗散孤子脉冲。

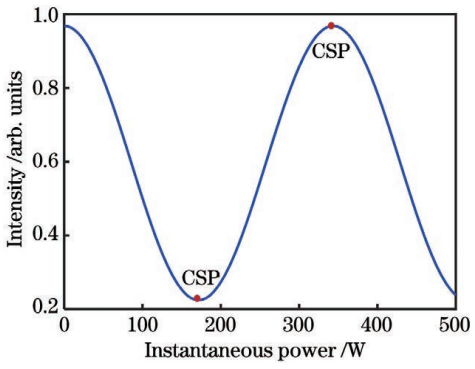

图 5 瞬时功率与非线性偏振旋转透过率关系曲线

Fig. 5 Relationship between instantaneous power and transmittance of nonlinear polarization rotation

值得一提的是，由于掺镱光纤激光器具有较高的脉冲峰值功率，在较高泵浦功率的作用下，滤波器中非线性相移项可能对梳状滤波产生显著的影响，使得梳状滤波传输峰的位置发生漂移，进而改变锁模激光器的中心波长。但是实验中所使用的 Lyot 滤波器具有稳定的梳状滤波，非线性相移的变化没有影响滤波器传输峰的位置，使得泵浦功率在持续增加过程中，虽然激光器的脉冲态发生了切换，但中心波长几乎处于同一波长位置。这也说明了这种滤波器具有较高的可靠性，可以用来设计波长稳定的激光光源。

4 结 论

利用保偏 45°倾斜光纤光栅作为起偏器，设计出了一种具有紧凑结构的 Lyot 滤波器。将该滤波器作为光谱滤波器放置在全正色散的掺镱光纤激光器中，在 177 mW 的泵浦功率下，激光器实现了稳定的耗散孤子锁模，中心波长为 1038.82 nm，脉宽为 5.2 ps，脉冲重复频率为 28.44 MHz。此外，在

保持偏振控制器状态不变的情况下，通过将泵浦功率从 177 mW 连续增加到 691 mW，激光器的锁模脉冲态实现了耗散孤子脉冲—类噪声脉冲—耗散孤子脉冲的切换。该激光器脉冲态的切换仅需通过调节泵浦功率来实现，具有更高的可控性和精准性，具有成为紧凑型多功能光源的潜力。

参 考 文 献

[1] Zhu Y J, Cui Z K, Sun X N, et al. All-polarization-maintaining dual-wavelength mode-locked fiber laser based on macro-bending loss tuning[C]//CLEO: Science and Innovations 2020, May10-15 2020, Washington, DC, United States. Washington, DC: OSA, 2020: SW3R.3.

[2] Tamura K, Ippen E P, Haus H A, et al. 77-fs pulse generation from a stretched-pulse mode-locked all-fiber ring laser[J]. Optics Letters, 1993, 18(13): 1080-1082.

[3] Zhang Z, Oktem B, Ilday F Ö. All-fiber-integrated soliton-similariton laser with in-line fiber filter[J]. Optics Letters, 2012, 37(17): 3489-3491.

[4] Zhao L M, Tang D Y, Wu J. Gain-guided soliton in a positive group-dispersion fiber laser[J]. Optics Letters, 2006, 31(12): 1788-1790.

[5] Schibli T R, Minoshima K, Hong F L, et al. Frequency metrology with a turnkey all-fiber system [J]. Optics Letters, 2004, 29(21): 2467-2469.

[6] Unruh J R, Price E S, Molla R G, et al. Two-photon microscopy with wavelength switchable fiber laser excitation[J]. Optics Express, 2006, 14(21): 9825-9831.

[7] Shah L, Fermann M E. High power femtosecond fiber chirped pulse amplification system for high speed micromachining[J]. Journal of Laser Micro/Nanoengineering, 2006, 1(3): 176-180.

[8] Grelu P, Akhmediev N. Dissipative solitons for mode-locked lasers[J]. Nature Photonics, 2012, 6(2): 84-92.

[9] Chong A, Buckley J, Renninger W, et al. All-normal-dispersion femtosecond fiber laser[J]. Optics Express, 2006, 14(21): 10095-10100.

[10] Li M, Zou X, Qiu J F, et al. Tunable multi-wavelength dissipative soliton generation in an Yb-doped fiber laser based on SESAM and Lyot-Sagnac filter[C]//2015 Opto-Electronics and Communications Conference (OECC), June 28-July 2, 2015, Shanghai, China. New York: IEEE Press, 2015: 1-3.

[11] Zhang L, Feng Y, Gu X J. Wavelength-switchable dissipative soliton fiber laser with a chirped fiber grating stop-band filter[J]. IEEE Photonics Journal, 2013, 5(2): 1500506.

[12] Ozgören K, Ilday F O. All-fiber all-normal dispersion laser with a fiber-based Lyot filter[J]. Optics Letters, 2010, 35(8): 1296-1298.

[13] Lin H Q, Guo C Y, Ruan S C, et al. Tunable and switchable dual-wavelength dissipative soliton operation of a weak-birefringence all-normal-dispersion Yb-doped fiber laser[J]. IEEE Photonics Journal, 2013, 5(5): 1501807.

[14] Zhang Z X, Dai G X. All-normal-dispersion dissipative soliton ytterbium fiber laser without dispersion compensation and additional filter[J]. IEEE Photonics Journal, 2011, 3(6): 1023-1029.

[15] Suzuki M, Ganeev R A, Yoneya S, et al. Generation of broadband noise-like pulse from Yb-doped fiber laser ring cavity[J]. Optics Letters, 2015, 40(5): 804-807.

[16] Zhao Y W, Zhao D S, Liu R M, et al. Switchable generation of a sub-200 fs dissipative soliton and a noise-like pulse in a normal-dispersion Tm-doped mode-locked fiber laser[J]. Applied Optics, 2020, 59(12): 3575-3581.

[17] Cheng X, Huang Q Q, Huang Z N, et al. Multi-shuttle behavior between dissipative solitons and noise-like pulses in an all-fiber laser[J]. Journal of Lightwave Technology, 2020, 38(8): 2471-2476.

[18] Sobon G, Sotor J, Martynkien T, et al. Ultra-broadband dissipative soliton and noise-like pulse generation from a normal dispersion mode-locked Tm-doped all-fiber laser[J]. Optics Express, 2016, 24(6): 6156-6161.

[19] Li X L, Zhang S M, Han M M, et al. Transformation from dissipative solitons to noise-like pulses in a mode-locked Yb-doped fiber laser[C]//Conference on Lasers and Electro-Optics/Pacific Rim 2018, July 29-August 3, 2018, Hong Kong, China. Washington, DC: OSA, 2018: W3A.64.

[20] Yan Z J, Zhou K M, Zhang L. In-fiber linear polarizer based on UV-inscribed 45° tilted grating in polarization maintaining fiber[J]. Optics Letters, 2012, 37(18): 3819-3821.

[21] Yan Z J, Wang H S, Zhou K M, et al. Broadband tunable all-fiber polarization interference filter based on 45° tilted fiber gratings[J]. Journal of Lightwave Technology, 2013, 31(1): 94-98.

[22] Zhang Z X, Xu Z W, Zhang L. Tunable and switchable dual-wavelength dissipative soliton generation in an all-normal-dispersion Yb-doped fiber laser with birefringence fiber filter[J]. Optics Express, 2012, 20(24): 26736-26742.

[23] Chong C Y. Femtosecond fiber lasers and amplifiers

based on the pulse propagation at normal dispersion [D]. Ithaca: Cornell University, 2008.

[24] Tang D Y, Zhao L M, Zhao B, et al. Mechanism of multisoliton formation and soliton energy quantization in passively mode-locked fiber lasers [J]. Physical Review A, 2005, 72(4): 043816.

Pulse State Switchable Ytterbium-Doped Fiber Laser Based on Lyot Filter

Lin Yanlü[1,2,3], Huang Zinan[1,2,3], Huang Qianqian[1,2,3], Dai Lilong[1,2,3], Xing Zhikun[4], Yan Zhijun[4], Mou Chengbo[1,2,3*]

[1] *Key Laboratory of Specialty Fiber Optics and Optical Access Networks, School of Communication & Information Engineering, Shanghai University, Shanghai* 200444, *China*;

[2] *Shanghai Institute for Advanced Communication and Data Science, Shanghai University, Shanghai* 200444, *China*;

[3] *Joint International Research Laboratory of Specialty Fiber Optics and Advanced Communication, Shanghai University, Shanghai* 200444, *China*;

[4] *National Engineering Laboratory for Next Generation Internet Access System, School of Optical and Electronic Information, Huazhong University of Science and Technology, Wuhan, Hubei* 430074, *China*

Abstract

Objective Various pulse shaping processes, including convention soliton, stretched pulse, similarity, and dissipative soliton, are formed in present passively mode-locked fiber lasers based on the diverse distribution positions of dispersion in the cavity. The development of soliton pulses has raised the single pulse energy to a new level, making fiber lasers cater to the needs of fields, such as optical metrology, biomedicine, and laser micromachining. Dissipative solitons are usually generated from lasers with a large net normal dispersion owing to the effects of dispersion, nonlinearity, gain, and loss. The spectral amplitude modulation introduced by the spectral filter plays a key role in forming the dissipative soliton. Therefore, various filters are used in the lasers. The birefringent filter has been widely used owing to its flexible filtering bandwidth and good fiber compatibility. In addition, noise-like pulses have also been extensively studied in normal dispersion lasers.

Both dissipative solitons and noise-like pulses can be generated in Ytterbium (Yb)-doped fiber lasers by reasonably adjusting the cavity parameters such as the pump power. Although pulse state switching has been verified in many experiments, few reports on the multiple switching of dissipative soliton and noise-like pulses in Yb-doped fiber lasers are available. In this study, we design a Lyot filter with a stable and powerful comb filtering using a pair of polarization-maintaining 45° tilted fiber gratings as polarizers and section of polarization-maintaining fiber as the birefringent medium. Therefore, an all-normal-dispersion Yb-doped fiber laser can achieve stable dissipative soliton mode-locking. By increasing the pump power unidirectionally in the dissipative soliton mode-locking state, the laser realizes multiple switching of dissipative soliton and noise-like pulse.

Methods Two polarization-maintaining 45° tilted fiber gratings are separated by a length of polarization-maintaining fiber with a particular splicing angle in the Lyot filter used in the experiment. It can be used as a comb filter in the laser cavity and a fiber-type polarizer because of its unique structure. To generate linear polarization light, the first grating couples the TE polarization component out of the fiber core and causes the TM polarization component to propagate in the fiber core. Linear polarization light accumulates linear phase shift in the polarization-maintaining fiber owing to the particular splicing angle between the grating and the polarization-maintaining fiber. The linear phase shift is transferred to the amplitude modulation in the second grating, resulting in comb filtering. The specific splicing angle is designed to be 45° for the filter to have the maximum-filtering modulation depth.

Results and Discussions The laser realizes stable dissipative soliton mode-locking with a pump power of 177 mW by finely adjusting the polarization controller, and its spectrum is shown in Fig. 4(a). The switching of the mode-locking pulse state can be observed while keeping the polarization controller and only increasing the pump power. When the pump power is increased to 323 mW, the spectrum gradually broadens under the influence of enhanced self-phase modulation. At this time, the pulse generated by the laser is still a dissipative soliton. Then, the pump power is continuously increased up to 455 mW in Fig. 4(e).

The sharp edges of the spectrum gradually disappear and become smooth. The autocorrelation trace in Fig. 4(f) has a wide base with a narrow peak, typical of noise-like pulses, indicating that the laser is working in a noise-like pulse regime. When the increasing pump power reaches 691 mW, the laser generates a dissipative soliton pulse again. The pulsed state switching of the laser can be attributed to the switching of the feedback mechanism of nonlinear polarization rotation. Fig. 5 shows the relationship between the instantaneous power and nonlinear polarization rotation transmittance. The sinusoidal transmission spectrum indicates that the nonlinear polarization rotation can occur in positive and negative states. The critical power of positive and negative feedback is named critical saturation power. After achieving stable mode-locking, the intracavity instantaneous power increases owing to the continuously increasing pump power. When the instantaneous power in the cavity exceeds the critical saturation power, the feedback mechanism of nonlinear polarization rotation switches from positive to negative feedback state, which causes the pulse state of the laser to switch from dissipative soliton to noise-like pulse. When the instantaneous power reaches the critical saturation power again, the feedback mechanism switches from the negative feedback state to the positive feedback state, so that the mode-locked pulse state of the laser also switches back to the dissipative soliton.

Conclusions We integrated a compact Lyot filter with a pair of polarization-maintaining 45° inclined fiber gratings in an all-normal-dispersion Yb-doped fiber laser. The laser realizes stable dissipative soliton mode-locking at a pump power of 177 mW. Furthermore, the pulse state of the laser recognizes switching from dissipative soliton to noise-like pulse and then to dissipative soliton by only continuously increasing the pump power from 177 mW to 691 mW. As adjusting the state of the polarization controller during switching is not necessary, it has higher controllability and accuracy, and the laser can be designed as a compact multifunctional light source.

Key words gratings; beam propagation; tilted fiber grating; Yb-doped fiber laser; nonlinear polarization rotation; dissipative soliton

OCIS codes 050.2770; 140.3615; 190.3270; 190.7110